



Structural, electronic and magnetic properties of neutral and anionic $\text{Fe}_2(\text{BO}_2)_n$ ($n = 1-3$) clusters



Hong Min Zhao^a, Xia Lin^a, Yawei Li^{b,c}, Qian Wang^{c,d,*}, Puru Jena^d

^a Department of Physics, School of Science, Beijing Jiaotong University, Beijing 100044, China

^b Department of Materials Science and Engineering, College of Engineering, Peking University, Beijing 100871, China

^c Center for Applied Physics and Technology, College of Engineering, Peking University, Beijing 100871, China

^d Department of Physics, Virginia Commonwealth University, Richmond, VA 23284, USA

ARTICLE INFO

Article history:

Received 8 May 2014

Received in revised form 7 August 2014

Accepted 12 August 2014

Available online 19 August 2014

Communicated by R. Wu

ABSTRACT

Using Fe_2 dimer as a prototype of transition-metal cluster calculations based on density functional theory have been carried out to study the effect of ligand and charge states on the geometry, bonding feature and magnetic coupling of neutral and anionic $\text{Fe}_2(\text{BO}_2)_n$ ($n = 1-3$) clusters. For neutral $\text{Fe}_2(\text{BO}_2)_n$ clusters the spin multiplicity of the complex changes from 7 to 8 when n goes from 0 to 1, 2, and 3. With increasing number of ligands the Fe–Fe distance increases, the magnetic coupling between Fe–Fe changes from direct exchange to super exchange, and 3d–2p hybridization between Fe and O atoms becomes predominant. For anionic $\text{Fe}_2(\text{BO}_2)_n$ ($n = 1-3$) clusters, the corresponding total magnetic moment is 0, 7 and $6\mu_B$, respectively. Compared with neutral clusters the HOMO–LUMO gaps of anionic species increase rapidly as more BO_2 units are introduced. This study sheds light on the potential of superhalogens to tune electronic and magnetic properties of Fe clusters.

© 2014 Published by Elsevier B.V.

1. Introduction

In the past decades, small iron clusters have drawn considerable attention both experimentally and theoretically due to their unique size-dependent electronic [1–3], magnetic [4–6] and catalytic [7,8] properties. Among the studied systems, the interaction of iron clusters with halogen atoms is of particular interest [9–11] due to the following reasons: (1) Fe_mCl_n species is an important model system with ferric active sites [12] existing in various proteins and enzymes. Studying these species is helpful to understand the role of Fe cations played in diverse biological processes. (2) Analysis of the underlying energetics and electronic structures of these species may enable one to understand the relationship between the halogen content and the formal valence of transition metal. Superhalogen moieties [13] with electron affinities substantially higher than that of Cl are of particular interest because they can promote chemical reaction otherwise inaccessible to halogens [14]. Among many superhalogen moieties, BO_2 [15] is interesting not only because it is halogen-free but also because it has a simple linear structure. Furthermore, BO_2^- is isoelectronic with CO_2 .

Recently a single Fe atom binding to multiple BO_2 ligands [16] and a single BO_2 ligand binding to Fe_n clusters ($n = 1-5$) [17]

have been studied by using photoelectron spectroscopy and density functional theory (DFT)-based calculations. However, studies exploring the possibility of inducing magnetic transition in Fe_n clusters through BO_2 ligand are lacking. In this paper we use Fe_2 as a prototype cluster to study how the electronic and magnetic properties change with the number of BO_2 ligands in both neutral and anionic states. Previous DFT calculations revealed that the magnetic coupling between two Mn atoms in Mn_2 can be effectively tuned by adding a bridged BO_2 ligand [18]. The study on Fe_2 counterpart would provide further information on the tuning ability of superhalogens for changing the properties of nanostructures.

2. Computational model and method

Calculations were performed using density functional theory (DFT) with B3LYP hybrid exchange–correlation functional and 6-311 + G(d) basis set [19–21] implemented in Gaussian 09 program [22]. The ground state structures and the corresponding spin states for all the neutral and negatively charged $\text{Fe}_2(\text{BO}_2)_n$ ($n = 1-3$) clusters were determined without any symmetry constraint. Tight convergence criteria were applied and several initial structures including all possible spin states were tried to determine the lowest energy and preferred magnetic structures for each species. Furthermore, harmonic vibrational frequencies were calculated to confirm the dynamic stability of the structures. Zero point energy (ZPE) corrections were applied to calculate total electronic

* Corresponding author at: Center for Applied Physics and Technology, College of Engineering, Peking University, Beijing 100871, China.

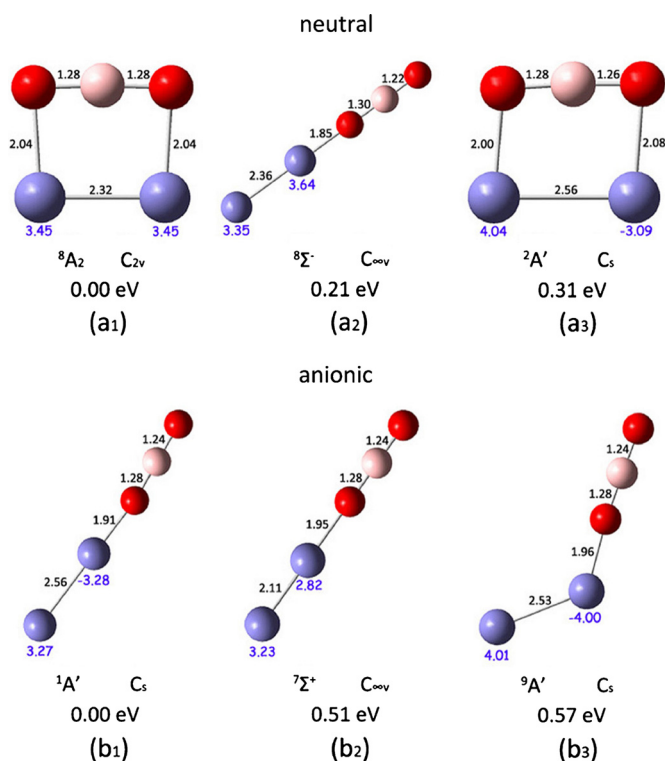


Fig. 1. Optimized structures of the low lying isomers of neutral (a₁–a₃) and anionic (b₁–b₃) Fe₂(BO₂)₂ clusters, and their corresponding ZPE corrected relative energies, electronic states as well as the point group symmetries at B3LYP/6-311 + G(d) level of theory. The bond lengths are given in Å and the magnetic moments of Fe atoms are given in μ_B .

energies. For each anionic species, we have calculated vertical detachment energy (VDE, the energy difference between the ground state of the anion and its neutral having the geometry of the anion ground state) as well as adiabatic detachment energy (ADE, the energy difference between the ground state of the anion and the neutral with the geometry close to that of the anion ground state). We also calculated electron affinity (EA) defined as the energy difference between ground states of anionic and neutral clusters. Natural bonding orbital (NBO) analyses [23,24] were carried out to elucidate the bonding patterns and the underlying mechanisms of the magnetic coupling in these clusters.

3. Results and discussions

3.1. Geometry, electronic structure, and magnetic properties

The ground state structures as well as the low-lying isomers of both neutral and anionic Fe₂(BO₂)₂ clusters are given in Fig. 1. The ground state of neutral Fe₂(BO₂)₂ has BO₂ in a bridged configuration with C_{2v} symmetry [see Fig. 1(a₁)]. The most preferred spin multiplicity of neutral Fe₂(BO₂)₂ is an octet with both the Fe atoms coupled ferromagnetically. Each Fe atom carries a magnetic moment of 3.45 μ_B . The Fe–Fe bond length is 2.32 Å. Note that each Fe site in bare Fe₂ carries a magnetic moment of 3 μ_B with the Fe–Fe bond length of 2.02 Å. Thus, the attachment of BO₂ enhances the moment and enlarges the Fe–Fe bond length.

There are two low-lying energy isomers of the neutral species. The first one has a linear configuration [see Fig. 1(a₂)] where the total magnetic moment is same as that of the ground state, but the two Fe sites have different moments, namely, 3.35 μ_B and 3.64 μ_B respectively. The Fe–Fe bond length is further increased to 2.36 Å. This isomer is 0.21 eV higher in energy as compared to the ground state. The second isomer with C_s symmetry is 0.31 eV higher in

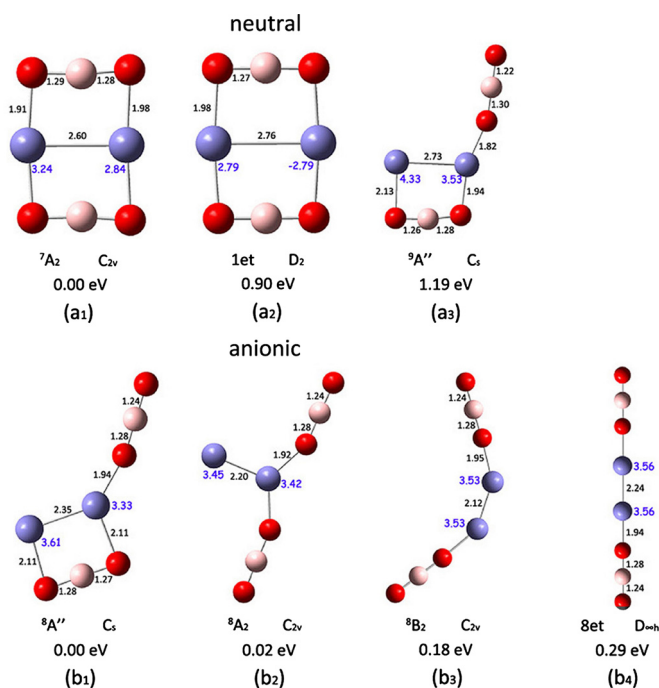


Fig. 2. Optimized structures of the low lying isomers of neutral (a₁–a₃) and anionic (b₁–b₃) Fe₂(BO₂)₂, and their corresponding ZPE corrected relative energies, electronic states as well as the point group symmetries at B3LYP/6-311 + G(d) level of theory. The bond lengths are given in Å and the magnetic moments of Fe atoms are given in μ_B .

energy and BO₂ is asymmetrically bonded to two Fe atoms [see Fig. 1(a₃)]. The slight change in bonding configuration results in an antiferromagnetic (AFM) state, showing the sensitivity of magnetic coupling to geometrical configuration.

For the negatively charged Fe₂BO₂ cluster, however, the BO₂ unit prefers to bind to one end of the Fe₂ dimer, generating a slightly distorted linear structure with the two Fe atoms coupled antiferromagnetically [see Fig. 1(b₁)]. This is the lowest energy structure. The next higher energy isomer is linear with septet spin multiplicity and lying 0.51 eV higher in energy [see Fig. 1(b₂)]. The Fe–Fe bond length of the AFM ground state is same as that of the AFM bridged isomer of neutral Fe₂(BO₂)₂ shown in Fig. 1(a₃). The nonet isomer with a bent geometry [see Fig. 1(b₃)] is energetically nearly degenerate with the linear septet isomer [see Fig. 1(b₂)]. We can see that the magnetic coupling is very sensitive to the bonding angle between Fe₂ and BO₂. This may be used as a strategy to specify the geometric configuration using magnetic measurements. It is also interesting to note that the preferred bridged configuration of neutral Fe₂(BO₂)₂ becomes energetically unfavorable in the anionic case which lies 0.6 eV higher in energy as compared to its ground state. The change of geometry and magnetic coupling of the ground state of anionic Fe₂(BO₂)₂[−] from that of its neutral cluster results in a noticeable difference between the VDE (1.73 eV), ADE (1.56 eV) and EA (1.35 eV) listed in Table 1. The large structural relaxation accounts for the observed broad band vibrational feature in the experimental Fe₂(BO₂)₂[−] PES spectrum [17].

When a second BO₂ is attached, the lowest energy structure of neutral Fe₂(BO₂)₂ adopts a double-bridged planar structure with C_{2v} symmetry, as shown in Fig. 2(a₁). Here the two Fe atoms are 2.60 Å apart and couple ferromagnetically with a total magnetic moment of 6 μ_B . An AFM isomer with a similar double-bridged structure having D₂ symmetry, as shown in Fig. 2(a₂), is higher in energy by 0.90 eV, suggesting that the FM coupling in neutral Fe₂(BO₂)₂ cluster is quite stable. The structures having one or two BO₂ ligands attached with an end-on configuration are more than 1.00 eV higher in energy compared to the ground state [see

Table 1
VDE, ADE, EA, and HOMO–LUMO gaps of the anionic and neutral $\text{Fe}_2(\text{BO}_2)_n$ ($n = 1–3$) clusters.

Cluster	Isomer	VDE (eV)	ADE (eV)	EA (eV)	HOMO–LUMO gap (eV)
Fe_2BO_2	neutral	1(a ₁)		1.35	1.87
	anionic	1(b ₁)	1.73	1.56	1.93
$\text{Fe}_2(\text{BO}_2)_2$	neutral	2(a ₁)		1.45	2.89
	anionic ^a	2(b ₁)	3.35	2.67	2.66
		2(b ₂)	3.49	/	2.66
		2(b ₃)	3.29	2.89	1.74
$\text{Fe}_2(\text{BO}_2)_3$	neutral	3(a ₁)		2.06	2.92
	anionic	3(b ₁)	3.86	2.06	3.56

^a There are three possible candidates of the ground state of $\text{Fe}_2(\text{BO}_2)_2$ anion.

Fig. 2(a₃)]. We have also considered structures where two BO_2 moieties dimerize to form a B_2O_4 moiety. However, such structures possess considerably higher energies, and thus are not presented here.

Interestingly, when an electron is added to the neutral $\text{Fe}_2(\text{BO}_2)_2$ cluster, the ground state geometry differs substantially from that in the neutral case, as illustrated in Fig. 2(b₁)–(b₃). The most preferable structures consist of two energetically degenerate isomers with one or two BO_2 units in end-on configurations [see Fig. 2(b₁) and Fig. 2(b₂)]. Another *cis*-form isomer [see Fig. 2(b₃)] with two BO_2 units attached to the opposite ends of Fe_2 dimer is higher in energy only by 0.18 eV. As illustrated in previous studies, hybrid DFT calculations can only discern isomers with an energy difference of more than ~ 0.2 eV. Therefore, there are three possible candidates of the anionic $\text{Fe}_2(\text{BO}_2)_2$ ground state. Despite their structural diversity, the Fe–Fe couplings in all the studied isomers are FM with a total moment of $7\mu_B$. The calculated VDE of anionic $\text{Fe}_2(\text{BO}_2)_2$ cluster is 3.35 eV, 3.49 eV and 3.29 eV for the structures in Fig. 2(b₁) to (b₃), respectively. The ADEs of the isomers 2(b₁) and 2(b₃) are 2.67 eV and 2.89 eV. We find that the computed EA is only 1.45 eV, suggesting that the neutral $\text{Fe}_2(\text{BO}_2)_2$ is electronically stable.

When a third BO_2 is attached to form $\text{Fe}_2(\text{BO}_2)_3$, we obtain different ground state geometries for neutral and anionic $\text{Fe}_2(\text{BO}_2)_3$ clusters. The lowest energy structure of neutral $\text{Fe}_2(\text{BO}_2)_3$ has a C_{2v} symmetry which is a planar structure with two BO_2 units in side-on configuration and one in an end-on configuration [see Fig. 3(a₁)]. The total magnetic moment of the ground state of neutral $\text{Fe}_2(\text{BO}_2)_3$ cluster is $7\mu_B$, and Fe sites carry magnetic moments of $3.00\mu_B$ and $3.81\mu_B$. The coupling is ferromagnetic. In this case, the Fe–Fe bond is broken with a distance of 4.32 Å. When all the three BO_2 units are bonded to Fe_2 in bridge configuration [see Fig. 3(a₂)], the Fe–Fe bond is still kept with a moment of $3.39\mu_B$ on each Fe site; however, this configuration is 0.46 eV higher in energy as compared to the first one. When changing the symmetry of C_{2v} in Fig. 3(a₁) to C_s in Fig. 3(a₃), the magnetic coupling switches from FM to AFM. Here we again witness the sensitivity of magnetism to symmetry.

For the anionic $\text{Fe}_2(\text{BO}_2)_3$ cluster, the feature of the ground state geometry [see Fig. 3(b₁)] is similar to that of its neutral counterpart, but the Fe–Fe distance is shortened to 2.94 Å, and spin multiplicity is reduced to 7 due to the added charge, and the structure becomes non-planar because of the charge-induced Jahn–Teller distortion. This structure is 0.21 eV lower in energy compared to the isomer plotted in Fig. 3(b₂), which is similar to the structure in Fig. 3(a₂) but for an 8% enlarged Fe–Fe distance. When two BO_2 moieties are in end-on configuration and one BO_2 is in bridge configuration [see Fig. 3(b₃)] the energy is 0.73 eV higher compared to the ground state. Although the studied three isomers of $\text{Fe}_2(\text{BO}_2)_3$ anion have different geometries, the couplings between Fe–Fe are all ferromagnetic, resulting in total moment of $6\mu_B$.

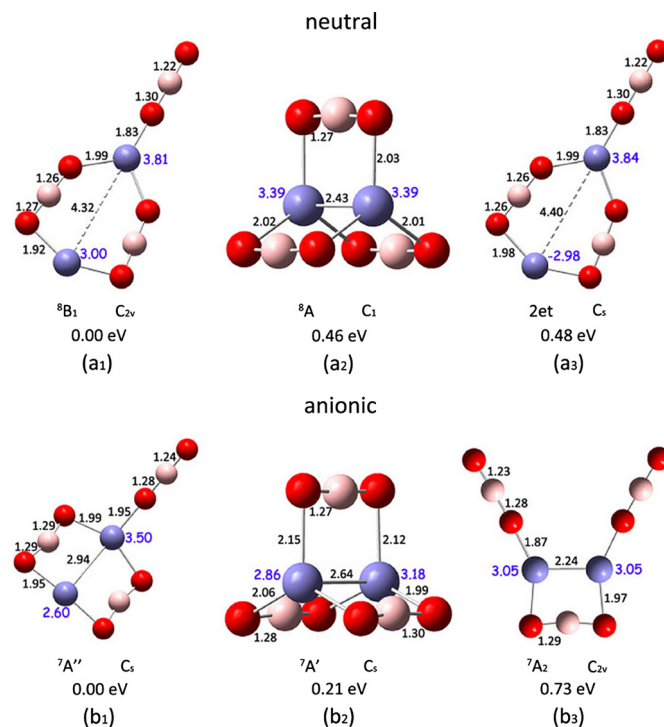


Fig. 3. Optimized structures of the low lying isomers of neutral (a₁–a₃) and anionic (b₁–b₃) $\text{Fe}_2(\text{BO}_2)_3$, and their corresponding ZPE corrected relative energies, electronic states as well as the point group symmetries at B3LYP/6-311 + $G(d)$ level of theory. The bond lengths are given in Å and the magnetic moments of Fe atoms are given in μ_B .

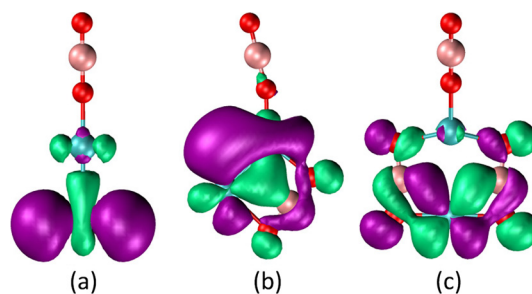


Fig. 4. HOMOs of the lowest energy structures of anionic (a) Fe_2BO_2 , (b) $\text{Fe}_2(\text{BO}_2)_2$ and (c) $\text{Fe}_2(\text{BO}_2)_3$. The isosurface value is set at $0.02 e/\text{Å}^3$.

Owing to the fact that the lowest energy structures of both anionic and neutral $\text{Fe}_2(\text{BO}_2)_3$ clusters are similar, the computed ADE of anionic $\text{Fe}_2(\text{BO}_2)_3$ and the theoretical EA of neutral species are exactly the same, namely 2.06 eV. On the other hand, the calculated VDE of the anionic $\text{Fe}_2(\text{BO}_2)_3$ cluster is as high as 3.86 eV, which corresponds to an electron detached from the spin-down channel. From the above analysis we can clearly see that none of

Table 2
NBO descriptors for the main bonding interactions of the Fe_2BO_2 , including symmetry type (sym) of bonding orbitals, occupancy (n_{occ}) of each bond, percentage of hybridization (h_a-h_b), polarization coefficients (pol) for α spin and β spin respectively.

Level of theory	$n_{\text{occ}}, h_a-h_b, \text{pol}$							
	α spin				β spin			
	sym	n_{occ}	h_a-h_b	pol	sym	n_{occ}	h_a-h_b	pol
B3LYP	$\sigma_{\text{Fe-Fe}}$	0.99	$sp^{0.10}d^{0.01}-sp^{0.10}d^{0.01}$	50.0–50.0	$\sigma_{\text{Fe-Fe}}$	1.00	$sp^{0.10}d^{0.52}-sp^{0.10}d^{0.52}$	50.0–50.0
					$\sigma_{\text{Fe-Fe}}$	1.00	$sp^{0.58}d^{99.9}-sp^{0.58}d^{99.9}$	50.0–50.0
					$\pi_{\text{Fe-Fe}}$	0.99	$p^{1.00}d^{31.6}-p^{1.00}d^{31.6}$	50.0–50.0
					$\pi_{\text{Fe-Fe}}$	0.92	$sp^{0.19}d^{7.41}-sp^{0.19}d^{7.41}$	50.0–50.0
Hartree-Fock	$\sigma_{\text{Fe-Fe}}$	1.00	$sp^{0.14}d^{0.01}-sp^{0.14}d^{0.01}$	50.0–50.0	$\sigma_{\text{Fe-Fe}}$	1.00	$sp^{0.19}d^{0.24}-sp^{0.19}d^{0.24}$	50.0–50.0
					$\sigma_{\text{Fe-Fe}}$	1.00	$sp^{1.80}d^{39.0}-sp^{1.80}d^{39.0}$	50.0–50.0
					$\pi_{\text{Fe-Fe}}$	0.98	$p^{1.00}d^{1.25}-p^{1.00}d^{1.25}$	50.0–50.0
					$\pi_{\text{Fe-Fe}}$	0.88	$sp^{1.29}d^{7.86}-sp^{1.29}d^{7.86}$	50.0–50.0
MP2	$\sigma_{\text{Fe-Fe}}$	1.00	$sp^{0.08}-sp^{0.08}$	50.0–50.0	$\sigma_{\text{Fe-Fe}}$	1.00	$sp^{0.09}d^{0.44}-sp^{0.09}d^{0.44}$	50.0–50.0
					$\sigma_{\text{Fe-Fe}}$	1.00	$sp^{0.83}d^{78.8}-sp^{0.83}d^{78.8}$	50.0–50.0
					$\pi_{\text{Fe-Fe}}$	0.99	$p^{1.00}d^{25.0}-p^{1.00}d^{25.0}$	50.0–50.0
					$\pi_{\text{Fe-Fe}}$	0.89	$sp^{0.30}d^{7.56}-sp^{0.30}d^{7.56}$	50.0–50.0
MP4 (SDQ)	$\sigma_{\text{Fe-Fe}}$	0.98	$sp^{0.08}-sp^{0.08}$	50.0–50.0	$\sigma_{\text{Fe-Fe}}$	1.00	$sp^{0.10}d^{0.46}-sp^{0.10}d^{0.46}$	50.0–50.0
					$\sigma_{\text{Fe-Fe}}$	1.00	$sp^{0.78}d^{81.5}-sp^{0.78}d^{81.5}$	50.0–50.0
					$\pi_{\text{Fe-Fe}}$	0.99	$p^{1.00}d^{25.6}-p^{1.00}d^{25.6}$	50.0–50.0
					$\pi_{\text{Fe-Fe}}$	0.90	$sp^{0.28}d^{7.51}-sp^{0.28}d^{7.51}$	50.0–50.0

the computed EAs of neutral $\text{Fe}_2(\text{BO}_2)_n$ ($n = 1-3$) clusters exceed the EA of a Cl atom (3.617 eV). Therefore, they don't belong to the category of superhalogens. However, when BO_2 moieties are increased from 1 to 3, the VDE values increase dramatically from 1.73 eV to 3.35 eV and to 3.86 eV. Such variation can be interpreted in a canonical molecular orbital perspective as discussed below. The highest occupied molecular orbitals (HOMOs) of anionic $\text{Fe}_2(\text{BO}_2)_n$ ($n = 1-3$) clusters are presented in Fig. 4. It is clear that in the HOMO of anionic Fe_2BO_2 cluster, electron density is strongly localized on the Fe atom that is not attached to a BO_2 moiety and exhibits mainly d_{z^2} character. On the other hand, the extent of electron delocalization is reinforced and such delocalization comprises almost all the atoms except for the end-on BO_2 unit in the HOMO of anionic $\text{Fe}_2(\text{BO}_2)_3$. Such electron delocalization between Fe atoms and bridged BO_2 ligands stabilizes the excess negative charge, rendering it more difficult for the negative charge to detach from anionic $\text{Fe}_2(\text{BO}_2)_3$ cluster and thus increasing the VDE.

3.2. Natural bonding orbital (NBO) analysis

In order to get a deeper insight into the bonding nature as well as the evolution of magnetic properties of $\text{Fe}_2(\text{BO}_2)_n$ ($n = 1-3$) clusters, we employed natural bond orbital (NBO) analysis implemented in NBO 3.1 program [25] of the Gaussian 09 package. This analyzes the electronic wave functions in the language of localized Lewis-like chemical bonds and extracts fundamental bonding features. We first used Fe_2BO_2 as an example to compare the NBO analysis using different levels of theory, including B3LYP, Hartree-Fock, MP2 and MP4. The calculated results are listed in Table 2, which shows that the orbital analysis generates basically the same results, although we found that the higher level calculations such as MP2 and MP4 give better single point energy value, but do not make much influence on NBO orbital analysis. The basic reason is that NBO analysis is based on proper sub-block density matrix and diagonalization, which are not very sensitive to the level of theory. Therefore, in the following we explain the bonding interactions through NBO analysis at B3LYP level.

The Fe-Fe bonding configurations for the six studied $\text{Fe}_2(\text{BO}_2)_n$ ($n = 1-3$) clusters are listed in Table 3. As we intend to use the NBO analysis to better understand the observed magnetic coupling between Fe atoms in $\text{Fe}_2(\text{BO}_2)_n$ ($n = 1-3$) clusters, only bonding orbitals consisting of Fe-Fe and Fe-O atoms are taken into account.

We have listed the symmetry type of each orbital which can be visualized in Figs. 5–7. Furthermore, the hybridization percentages of the interacting atoms are listed for identifying the main bonding interactions. We have set all the s (or p in cases where no s characters exist) character to 1 as a reference. For example, if the hybridization percentage of an oxygen atom is $sp^{12.3}$, it means that the percentage of p character is $12.3/(1 + 12.3) = 92.4\%$, suggesting that the oxygen atom mainly provides p electrons to form bonds with other atoms.

Our natural population analysis reveals that in anionic Fe_2BO_2 , the BO_2 unit carries a negative charge of $-0.89e$, indicating that the BO_2 unit draws the majority of the extra electron to itself due to its large electronegativity, namely, $[\text{Fe}_2\text{BO}_2]^- \sim \text{Fe}_2[\text{BO}_2]^-$, so it seems that the Fe_2 in anionic Fe_2BO_2 may exhibit similar magnetic properties as the neutral Fe_2 in a free state. However, this is not the case. The ground state of anionic Fe_2BO_2 is antiferromagnetic, different from the ferromagnetic coupling in Fe_2 dimer. To understand this unexpected result, we need to use NBO analysis. We see clearly from Table 3 that in anionic Fe_2BO_2 , the Fe-Fe bond is comprised of only σ bonding orbitals in both α spin and β spin channels with occupation number of 1.00, and the two σ spin orbitals exhibit primarily s atomic orbital character which is also confirmed from Fig. 5. The σ bonding orbital in α spin channel is contributed by two nonequivalent Fe atoms with the percentages of 80.2 and 19.8 due to its asymmetric configuration. The corresponding percentages in β spin channel are 59.2 and 40.8. So the d electrons in anionic Fe_2BO_2 cluster play a negligible role in Fe-Fe bonding interactions. This is very different from the case of Fe_2 molecule in a free state as shown in Fig. 5, where the d electrons participate in σ , π , and δ Fe-Fe bonding in β spin channel. Similar features can also be found in neutral Fe_2BO_2 cluster. It is the direct d-d interaction that yields the ferromagnetic coupling between the two Fe atoms in Fe_2 molecule as well as in neutral Fe_2BO_2 cluster. However, in anionic Fe_2BO_2 cluster, the strong direct d-d interactions are absent; the Fe-Fe magnetic coupling is mediated by s electrons which results in an antiferromagnetic coupling. This can be further verified by their electron configurations: in the spin-up channel: Fe1 ($4s^{0.81}3d^{4.97}$), Fe2 ($4s^{0.17}3d^{1.98}$), while in the spin-down channel: Fe1 ($4s^{0.67}3d^{1.90}$), Fe2 ($4s^{0.41}3d^{4.91}$). Therefore, the two Fe atoms are anti-ferromagnetically coupled.

The differences exhibited in anionic Fe_2BO_2 cluster as compared with its neutral counterpart and Fe_2 molecule can be further seen through the Wiberg bond indexes for the two Fe atoms: which

Table 3

NBO descriptors for the main bonding interactions of the $\text{Fe}_2(\text{BO}_2)_n$ ($n = 1-3$) clusters, including symmetry type (sym) of bonding orbitals, occupancy (n_{occ}) of each bond, percentage of hybridization (h_a-h_b), polarization coefficients (pol).

Isomer	$n_{\text{occ}}, h_a-h_b, \text{pol}$							
	α spin				β spin			
	sym	n_{occ}	h_a-h_b	pol	sym	n_{occ}	h_a-h_b	pol
1(a ₁)	$\sigma_{\text{Fe-Fe}}$	0.99	$sp^{0.10}d^{0.01}-sp^{0.10}d^{0.01}$	50.0–50.0	$\sigma_{\text{Fe-Fe}}$	1.00	$sp^{0.10}d^{0.52}-sp^{0.10}d^{0.52}$	50.0–50.0
					$\sigma_{\text{Fe-Fe}}$	1.00	$sp^{0.58}d^{99.9}-sp^{0.58}d^{99.9}$	50.0–50.0
					$\pi_{\text{Fe-Fe}}$	0.99	$p^{1.00}d^{31.6}-p^{1.00}d^{31.6}$	50.0–50.0
					$\pi_{\text{Fe-Fe}}$	0.92	$sp^{0.19}d^{7.41}-sp^{0.19}d^{7.41}$	50.0–50.0
1(b ₁)	$\sigma_{\text{Fe-Fe}}$	1.00	$sd^{0.03}-sp^{0.25}d^{0.04}$	80.2–19.8	$\sigma_{\text{Fe-Fe}}$	1.00	$sp^{0.01}d^{0.30}-sp^{0.20}d^{0.06}$	59.2–40.8
					$\pi_{\text{Fe-O}}$	0.92	$sp^{2.25}d^{14.8}-sp^{74.2}d^{0.02}$	2.4–97.6
2(a ₁)	/	/	/	/	$\sigma_{\text{Fe-O}}$	0.94	$sp^{8.03}d^{99.9}-sp^{12.3}$	17.3–82.7
					$\sigma_{\text{Fe-O}}$	0.94	$sp^{0.24}d^{35.6}-sp^{10.2}$	30.4–69.6
					$\sigma_{\text{Fe-O}}$	0.58	$sp^{0.24}d^{35.6}-sp^{10.2}$	69.6–30.4
2(b ₁)	$\sigma_{\text{Fe-Fe}}$	0.98	$sp^{0.04}-sp^{0.36}d^{0.02}$	76.8–23.2	$\sigma_{\text{Fe-Fe}}$	0.95	$sp^{0.12}d^{0.6}-sp^{0.48}d^{0.60}$	48.7–51.3
					$\pi_{\text{Fe-Fe}}$	0.75	$sp^{0.19}d^{2.18}-sp^{1.73}d^{3.72}$	63.8–36.2
3(a ₁)	/	/	/	/	$\sigma_{\text{Fe-O}}$	0.90	$sp^{0.43}d^{2.52}-sp^{21.9}d^{0.02}$	7.6–92.4
					$\sigma_{\text{Fe-O}}$	0.90	$sp^{0.43}d^{2.52}-sp^{21.9}d^{0.02}$	7.6–92.4
					$\sigma_{\text{Fe-O}}$	0.91	$sp^{1.08}d^{1.29}-sp^{20.1}$	5.2–94.8
3(b ₁)	/	/	/	/	$\sigma_{\text{Fe-O}}$	0.97	$sp^{0.40}d^{79.6}-sp^{8.41}$	38.6–61.4
					$\sigma_{\text{Fe-O}}$	0.63	$sp^{0.40}d^{79.6}-sp^{8.41}$	61.4–38.6
					$\sigma_{\text{Fe-O}}$	0.94	$sp^{1.60}d^{9.01}-sp^{9.69}$	11.6–88.4

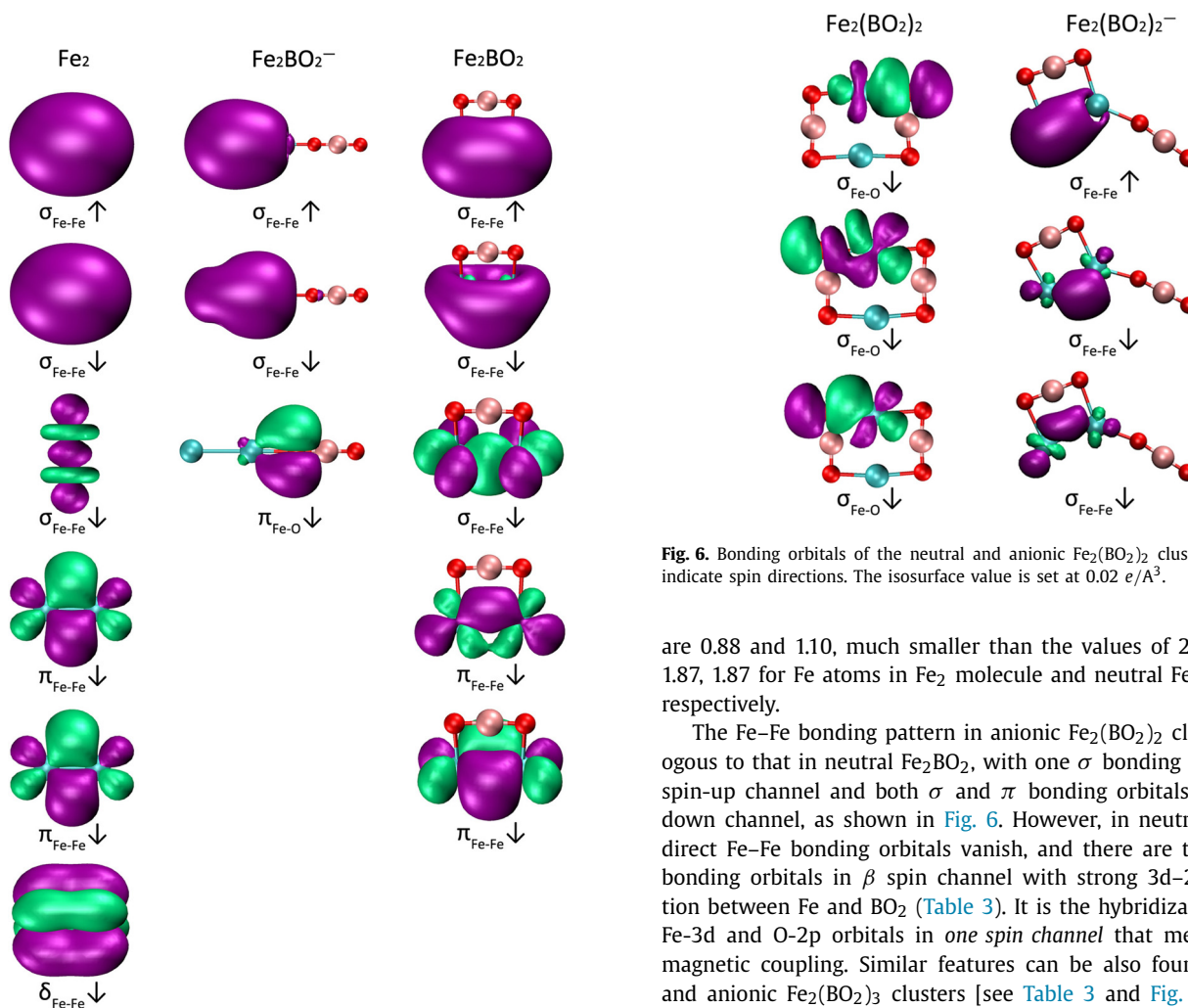


Fig. 5. Bonding orbitals of Fe_2 dimer, the anionic and neutral Fe_2BO_2 cluster. The arrows indicate spin directions. The isosurface value is set at $0.02 e/A^3$.

Fig. 6. Bonding orbitals of the neutral and anionic $\text{Fe}_2(\text{BO}_2)_2$ clusters. The arrows indicate spin directions. The isosurface value is set at $0.02 e/A^3$.

are 0.88 and 1.10, much smaller than the values of 2.01, 2.01 and 1.87, 1.87 for Fe atoms in Fe_2 molecule and neutral Fe_2BO_2 cluster, respectively.

The Fe–Fe bonding pattern in anionic $\text{Fe}_2(\text{BO}_2)_2$ cluster is analogous to that in neutral Fe_2BO_2 , with one σ bonding orbital in the spin-up channel and both σ and π bonding orbitals in the spin-down channel, as shown in Fig. 6. However, in neutral $\text{Fe}_2(\text{BO}_2)_2$, direct Fe–Fe bonding orbitals vanish, and there are three σ Fe–O bonding orbitals in β spin channel with strong 3d–2p hybridization between Fe and BO_2 (Table 3). It is the hybridization between Fe–3d and O–2p orbitals in *one spin channel* that mediates ferromagnetic coupling. Similar features can be also found in neutral and anionic $\text{Fe}_2(\text{BO}_2)_3$ clusters [see Table 3 and Fig. 7]. Based on above analysis and discussions, we see that the Fe–Fe magnetic coupling can be tuned from direct exchange to super exchange as more BO_2 units are attached to Fe_2 dimer.

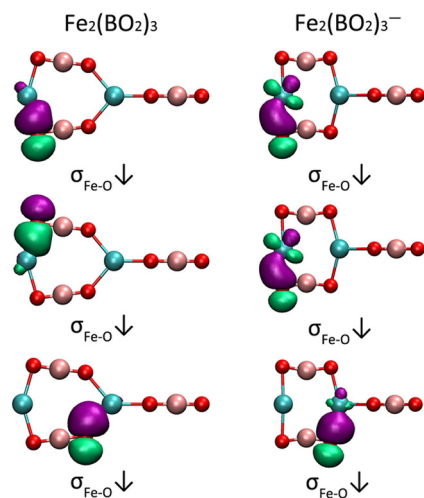


Fig. 7. Bonding orbitals of the neutral and anionic $\text{Fe}_2(\text{BO}_2)_3$. The arrows indicate spin directions. The isosurface value is set at $0.02 e/\text{\AA}^3$.

4. Conclusions

We have performed DFT calculations using B3LYP hybrid functional to investigate the geometries of neutral and anionic $\text{Fe}_2(\text{BO}_2)_n$ ($n = 1-3$) clusters as well as the bonding feature and magnetic coupling. The following conclusions can be drawn: (1) In the neutral complexes, BO_2 unit prefers the bridge configuration while in the anionic clusters the end-on configuration is energetically more favorable. (2) As more BO_2 units are attached to Fe_2 , the VDE, EA and HOMO-LUMO gap increase monotonically, while the EA values oscillate. (3) In the neutral clusters, the magnetic coupling between Fe-Fe atoms is ferromagnetic while in the anionic clusters, antiferromagnetic coupling may exist. (4) NBO analysis suggests that in the negatively charged Fe_2BO_2 cluster, Fe-Fe s orbital bonding plays a dominant role. In the neutral Fe_2BO_2 and negatively charged $\text{Fe}_2(\text{BO}_2)_2$, both Fe d-d bonding and s-s bonding are involved, while Fe-O d-p interactions are dominant in the remaining clusters.

Acknowledgements

This work is partially supported by grants from the Fundamental Research Funds for the Central Universities (2013JBM102), the National Natural Science Foundation of China (NSFC-11174014,

NSFC-21273012), the Doctoral Program of Higher Education of China (20130001110033), and the U.S. Department of Energy, Office of Basic Energy Sciences, Division of Materials Sciences and Engineering, under Award No. DEFG02-96ER45579.

References

- [1] L.S. Wang, H.S. Cheng, J. Fan, *J. Chem. Phys.* 102 (1995) 9480–9493.
- [2] L.-S. Wang, X. Li, H.-F. Zhang, *Chem. Phys.* 262 (2000) 53–63.
- [3] L.-S. Wang, H.-S. Cheng, J. Fan, *Chem. Phys. Lett.* 236 (1995) 57–63.
- [4] M. Wu, A.K. Kandalam, G.L. Gutsev, P. Jena, *Phys. Rev. B* 86 (2012) 174410.
- [5] P.G. Alvarado-Leyva, F. Aguilera-Granja, L.C. Balbas, A. Vega, *Phys. Chem. Chem. Phys.* 15 (2013) 14458–14464.
- [6] G.L. Gutsev, C.A. Weatherford, P. Jena, E. Johnson, B.R. Ramachandran, *J. Phys. Chem. A* 116 (2012) 10218–10228.
- [7] A.H. Pakiari, M. Mousavi, *J. Phys. Chem. A* 114 (2010) 10209–10216.
- [8] G.L. Gutsev, M.D. Mochena, C.W. Bauschlicher Jr., *Chem. Phys.* 314 (2005) 291–298.
- [9] D. Schröder, J. Loos, H. Schwarz, R. Thissen, O. Dutuit, *Inorg. Chem.* 40 (2001) 3161–3169.
- [10] L.-P. Ding, X.-Y. Kuang, P. Shao, M.-M. Zhong, Y.-R. Zhao, *J. Chem. Phys.* 139 (2013) 104304.
- [11] Y. Li, S. Zhang, Q. Wang, P. Jena, *J. Chem. Phys.* 138 (2013) 054309.
- [12] N. Oliphant, R.J. Bartlett, *J. Am. Chem. Soc.* 116 (1994) 4091–4092.
- [13] G.L. Gutsev, A.I. Boldyrev, *Chem. Phys.* 56 (1981) 277–283.
- [14] D. Samanta, P. Jena, *J. Am. Chem. Soc.* 134 (2012) 8400–8403.
- [15] H.-J. Zhai, L.-M. Wang, S.-D. Li, L.-S. Wang, *J. Phys. Chem. A* 111 (2007) 1030–1035.
- [16] P. Koirala, K. Pradhan, A.K. Kandalam, P. Jena, *J. Phys. Chem. A* 117 (2012) 1310–1318.
- [17] Y. Feng, H.-G. Xu, Z.-G. Zhang, Z. Gao, W. Zheng, *J. Chem. Phys.* 132 (2010) 074308.
- [18] M.M. Wu, Q. Wang, Q. Sun, P. Jena, *J. Phys. Chem. A* 115 (2010) 549–555.
- [19] A.D. Becke, *J. Chem. Phys.* 98 (1993) 5648–5652.
- [20] R. Krishnan, J.S. Binkley, R. Seeger, J.A. Pople, *J. Chem. Phys.* 72 (1980) 650–654.
- [21] A.D. McLean, G.S. Chandler, *J. Chem. Phys.* 72 (1980) 5639–5648.
- [22] M.J. Frisch, G.W. Trucks, H.B. Schlegel, G.E. Scuseria, M.A. Robb, J.R. Cheeseman, G. Scalmani, V. Barone, B. Mennucci, G.A. Petersson, H. Nakatsuji, M. Caricato, X. Li, H.P. Hratchian, A.F. Izmaylov, J. Bloino, G. Zheng, J.L. Sonnenberg, M. Hada, M. Ehara, K. Toyota, R. Fukuda, J. Hasegawa, M. Ishida, T. Nakajima, Y. Honda, O. Kitao, H. Nakai, T. Vreven, J.A. Montgomery Jr., J.E. Peralta, F. Ogliaro, M. Bearpark, J.J. Heyd, E. Brothers, K.N. Kudin, V.N. Staroverov, R. Kobayashi, J. Normand, K. Raghavachari, A. Rendell, J.C. Burant, S.S. Iyengar, J. Tomasi, M. Cossi, N. Rega, J.M. Millam, M. Klene, J.E. Knox, J.B. Cross, V. Bakken, C. Adamo, J. Jaramillo, R. Gomperts, R.E. Stratmann, O. Yazyev, A.J. Austin, R. Cammi, C. Pomelli, J.W. Ochterski, R.L. Martin, K. Morokuma, V.G. Zakrzewski, G.A. Voth, P. Salvador, J.J. Dannenberg, S. Dapprich, A.D. Daniels, O. Farkas, J.B. Foresman, J.V. Ortiz, J. Cioslowski, D.J. Fox, Gaussian 09, Revision A.02.
- [23] J.P. Foster, F. Weinhold, *J. Am. Chem. Soc.* 102 (1980) 7211–7218.
- [24] A.E. Reed, R.B. Weinstock, F. Weinhold, *J. Chem. Phys.* 83 (1985) 735–746.
- [25] E.D. Glendening, A.E. Reed, J.E. Carpenter, F. Weinhold, NBO Version 3.1.